Picosecond transient photoluminescence in high-density Si-nanodisk arrays fabricated using bio-nano-templates

Takayuki Kiba, Yoshiya Mizushima, Makoto Igarashi, Chi-Hsien Huang, Seiji Samukawa et al.

Citation: Appl. Phys. Lett. **100**, 053117 (2012); doi: 10.1063/1.3681793
View online: http://dx.doi.org/10.1063/1.3681793
View Table of Contents: http://apl.aip.org/resource/1/APPLAB/v100/i5
Published by the American Institute of Physics.

Picosecond transient photoluminescence in high-density Si-nanodisk arrays fabricated using bio-nano-templates

Takayuki Kiba,[1,2,a)] Yoshiya Mizushima,[1] Makoto Igarashi,[2,3] Chi-Hsien Huang,[2,3] Seiji Samukawa,[2,3] and Akihiro Murayama[1,2]
[1]*Graduate School of Information Science and Technology, Hokkaido University, Kita 14, Nishi 9, Kita-ku, Sapporo 060-0814, Japan*
[2]*Japan Science and Technology Agency, CREST, 5 Sanbancho, Chiyoda, Tokyo 102-0075, Japan*
[3]*Institute of Fluid Science, Tohoku University, 2-1-1 Katahira, Aoba-ku, Sendai 980-8577, Japan*

(Received 28 November 2011; accepted 14 January 2012; published online 2 February 2012)

We study picosecond transient photoluminescence (PL) in Si-nanodisk (Si-ND) arrays fabricated using bio-nano-templates. The PL time profiles show multi-exponential decaying kinetics depending on the disk density. We attribute the fastest decaying component with a decay time of 40 ps observed only in the high-density Si-ND array to the electron transfer among the Si-NDs. [doi:10.1063/1.3681793]

Si nanostructures have extensively been studied owing to their potential applications in future photovoltaics and optoelectronics.[1–11] Si nanostructures with dimensions of less than 10 nm can behave as quantum dots (QDs) due to a three-dimensional quantum confinement effect for carriers. Minibands of carriers will arise from overlapping of the confined wavefunctions in high-density QDs regularly aligned.[3,4] However, typical Si nanocrystals produced using conventional fabrication techniques show significant distributions in the shape, size, and spacing. Moreover, in these fabrication processes, a large amount of defect-induced local energy levels can be easily formed. As a result, the majority of experiments on Si nanostructures have shown extremely slow decaying photoluminescence (PL) with decay times up to a μs region,[5] which is not suitable for high-speed optical devices.

Recently, we have developed a fabrication process to realize high-density Si-nanodisk (ND) arrays by using bio-nano-templates and damage-free neutral beam (NB) etching.[12,13] This fabrication process allows us to design the precise size and spacing of the closely packed Si-NDs with flexible film stacking. Each wavefunction can spread over neighboring NDs in this periodic regular alignment of the ND with ultrathin potential barriers. Therefore, the carrier dynamics in this Si-ND array system needs to be clarified for the purpose of establishing ultrafast and, thus, efficient spatial separation of an electron and hole pair, which is important for solar cell applications.

Two-dimensional nearly closed-packed Si-ND arrays[12] embedded in SiO_2 were fabricated by using a combination of bio-nano-templates of ferritin supramolecules and subsequent defect-free NB etching. Details of the fabrication process are described elsewhere.[13,14] The ND diameter, thickness, and the interspacing were intentionally designed at 10, 8, and 2 nm, respectively, by this ferritin protein engineering. We prepared an isolated low-density ND sample whose average inter-disk distance was more than 40 nm, as a reference. To investigate the carrier dynamics in these Si-ND arrays, time-resolved PL spectra were observed at various excitation densities and temperatures. The samples were excited by second harmonic light pulses of a mode-locked Ti:sapphire laser with a wavelength of 400 nm, providing ultrashort pulses with a time width of 150 fs and a repetition rate of 76 MHz. The time-resolved PL spectra were detected by a synchroscan streak camera. The time width of the instrumental response curve was 15 ps.

Time-integrated PL spectrum of the Si-ND array at 150 K for an excitation power of 50 mW is shown in Fig. 1(a). PL emission bands centered at wavelengths of 665 nm (= 1.86 eV, E_1 band) and 555 nm (= 2.23 eV, E_2 band) are seen. No significant temperature and excitation-power dependences of the PL peak energy and spectral shape were observed. The PL intensity of the Si-ND array is plotted in Fig. 1(b) as a function of temperature. In a low temperature regime (10–150 K), the PL intensity increases with increasing temperature. The intensity peaks at a maximum between 150 and 200 K. The PL intensity then decreases monotonically with further increasing temperature from 250 to 300 K. We analyzed this temperature dependence of the PL intensity by using a thermal quenching model taking a lower energy level in addition to an emissive one into consideration.[15] The rapid decrease in the PL intensity from 250 to 300 K can be

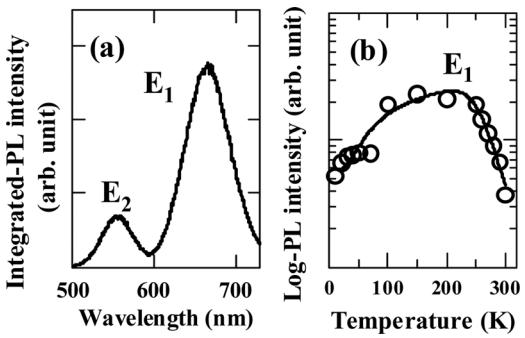

FIG. 1. (a) Typical time-integrated PL spectrum of the Si-ND array at 150 K with an excitation power of 50 mW. (b) The PL intensity of the Si-ND array for E_1 band indicated in (a) as a function of temperature. The solid line is a calculation.

[a)]Address to whom correspondence should be addressed. Electronic mail: tkiba@ist.hokudai.ac.jp. Tel/Fax: +81-11-706-6519.

well described by an activation energy of 0.32 eV, which is in good agreement with values of 0.22 – 0.31 eV obtained in our previous conductivity measurement for the same Si-ND array system.[16] This agreement directly shows that electrons transfer through barriers among NDs, without a significant loss or capture by defects.

First, we show results on the low-density Si-ND reference sample to clarify transient PL properties of individual isolated Si-NDs. We measured the PL time-profile for this low-density Si-ND sample at 150 K with various excitation powers from 2 to 50 mW (0.3 to 8.4 μJ cm^{-2}), as shown in Fig. 2(a). Fig. 2(b) shows a typical fitting result of the PL time-profile. Two PL components are identified with time constants $\tau_1 = 1.8$ ns and $\tau_2 = 130$ ps, where these values are almost constant for whole excitation-power range. This emission timescale is much faster than that of μs-scale emissions relating to defects reported in several studies of Si-nanocrystals.[5,8] Therefore, the present fast PL components originate from intrinsic states of the individual Si-NDs. The relative intensity ratios of these two PL components as a function of excitation power are shown in Fig. 2(c). The slower component A_1 (with τ_1) is always dominant in whole excitation-power range; meanwhile, the time-integrated faster component A_2 (with τ_2) shows only minor contribution to the PL intensity. Therefore, we assign the slower component to radiative recombination of photo-excited electron-hole pairs or excitons in individual NDs.

Next, the excitation-density dependence of the PL time-profile for the high-density Si-ND array sample is shown in Fig. 3(a) at 150 K by changing the excitation power from 2 to 50 mW. We measured also a μs-scaled PL time-profile of this Si-ND array by using laser pulses with the repetition rate of 1 kHz, as shown by an inset in Fig. 3(a). The PL emission decays instantaneously within the instrumental time resolution of 2 μs and no slow PL component in the μs range is detected. We conclude that there was no build-up of PL signal between the excitation pulses. Several fit routines were tested, including multi-exponential fit functions and stretched exponential functions to analyze these decay curves. The best fit was obtained with a triple exponential function, as shown in Fig. 3(b). The stretched exponential functions that were widely used to PL decay curves obtained from porous-Si or Si nanocrystals could not be applied here. The stretched exponential fitting corresponded to a broad distribution of decay times due to the dispersive motion of exciton in disordered systems. We have identified three PL decaying components with time constants $\tau_1 = 1.9$ ns, $\tau_2 = 320$ ps, and $\tau_3 = 40$ ps. The excitation-density dependence of this Si-ND array showed that each decay time was almost constant and the relative intensities of each decaying component changed. The contribution of faster two components (shaded area in Fig. 3(a)) increased markedly as the excitation-density increased. Fig. 3(c) shows the excitation-power dependence of the relative time-integrated intensity ratio of each decaying component. At lower excitation powers, most emissions arise with A_1 (with τ_1). It should be noted that the fastest component A_3 (with τ_3) was observed only in this high-density Si-ND array sample. This fact suggests that the τ_3 component represents an inherent process of the Si-ND array structure.

Three PL components with different decay times indicate that three different types of ND sites in the ND array emit PL with different decay-time constants. The decay time τ_1 on the order of 1 ns is interpreted by the formation of electron-hole pairs or excitons localized at individual NDs because of the same decay time τ_1 observed in the previous low-density Si-ND sample. This is also supported by the abovementioned excitation-power dependence of transient PL in the Si-ND array. In the array structure, each ND can be regarded as a localized potential minimum for carriers and a large number of vacant NDs exist at low excitation densities. Carriers relax immediately after the excitation to the lowest states of the ND array system, i.e., the "localized"

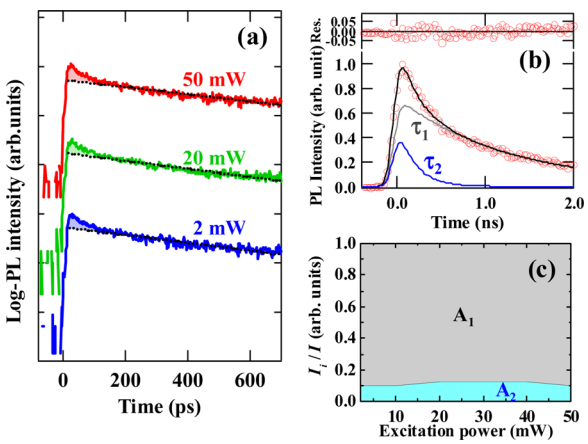

FIG. 2. (Color online) (a) Normalized PL time-profiles (log-scaled and vertically shifted) of the low-density Si-ND reference sample as a function of excitation power. A dashed black line shows a long-lived PL component. (b) Typical fitting result of the PL time-profile for the low-density Si-NDs at 50 mW and 150 K using a double exponential function, where the PL time-profile was deconvoluted with an instrumental response function. A bold black line shows a fitting calculation. The resolved decaying components with decay times of τ_1 and τ_2 are also shown by the narrow lines. (c) Excitation-power dependences of the relative time-integrated intensities A_1 and A_2, corresponding to the decaying components with τ_1 and τ_2.

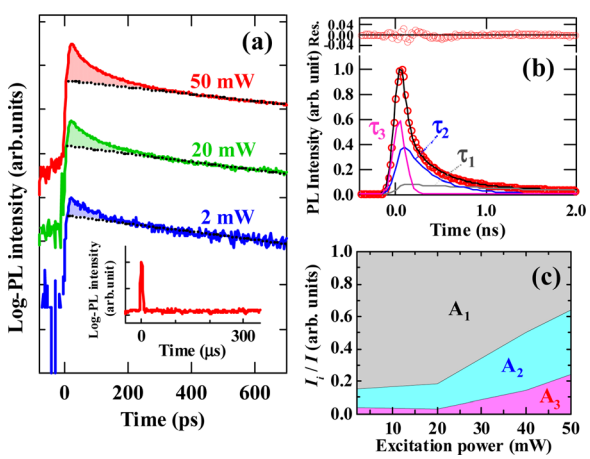

FIG. 3. (Color online) (a) Normalized PL time-profiles of the high-density Si-ND array as a function of excitation power. Inset shows a μs-scaled PL time-profile of the Si-ND array excited by laser pulses with the repetition rate of 1 kHz. (b) Typical fitting result of the PL time-profile of the Si-ND array at 50 mW and 150 K using a triple exponential function. The solid lines are fitting calculations. (c) Excitation-power dependences of the relative time-integrated intensities A_1, A_2, and A_3, corresponding to the decaying components with τ_1, τ_2, and τ_1.

states of the individual NDs. At higher excitation densities, this composition (A_1) decreases as compared to A_2 and A_3 due to a filling effect for the localized ND states, since the number of vacant ND is limited. The number of electron-hole pair generated per one ND is calculated with assuming the internal quantum efficiency of 1. The calculated number of generated carrier per ND is ranged from 0.072 (at 2 mW) to 1.8 (at 50 mW). Therefore, the filling effect observed in this excitation density range is justified.

We consider radiative recombination processes with time constants τ_2 and τ_3 based on a free-like electron-hole pair or exciton (not strongly localized in each ND) in the present highly ordered Si-ND array system, where each wavefunction spreads over neighboring NDs to some extent due to periodic regular alignment of the ND separated by ultrathin (2 nm) potential barriers of SiO_2. The carrier transfer among NDs can affect the PL decay time. If the transfer time is faster than a radiative lifetime, the shortened PL decay time can be observed. If an electron having the lighter effective mass than a hole can be transferred prior to the radiative recombination, the PL decay time approaches to the electron transfer time. The existence of transfer channel of electron in the present high-density Si-ND array is supported by the fact that the activation energy for the thermal quenching of PL is the same as that obtained from electron conductivity measurements. These considerations lead us to assume two types of arrangement of the ND-potential in the high-density Si-ND array system. The first arrangement consists of a ND adjoining one or more NDs with lower potentials, where the electron can move spatially due to the energy relaxation after the tunneling of the electron wavefunction through the barrier. This arrangement can induce the fastest emission with τ_3. This fastest component was actually observed only in the high-density Si-ND array sample. The second arrangement is a ND surrounded by other NDs with equal or higher potentials. In this case, the electron cannot move to the surrounding NDs. This corresponds to the emission with τ_2. The decay time τ_2 is faster than τ_1, as the radiative lifetime of an electron-hole pair or exciton is shorter than that in a localized state (τ_1). In a system of GaAs, a PL decay times of weekly localized excitons in a quantum well were reported to be in a order of several hundred ps,[17] while those of strongly localized excitons in a quantum disk were about 1 ns.[18]

Tunneling rates of carriers were calculated using one-dimensional semi-classical model.[19,20] The activation energy of 0.32 eV determined from the temperature dependence of PL intensity was used as an effective height of the barrier for the electron. The calculated tunneling rate of electron is plotted as a function of barrier thickness in Fig. 4. The tunneling rate for the barrier thickness of 2 nm – designed value of this disk interval – is 6 ps, which is a little faster than the observed decay time τ_3. The transfer channel with the relatively low barrier height can be understood by quasi-miniband formation due to the regularly aligned periodic array of the present Si NDs with thin barrier layers of SiO_2, which is also interpreted as the first excited state of electron in the ND where the wavefunction penetrates into neighboring NDs. In addition to this, the band-gap energy of SiO_2 could be reduced by the existence of SiOH bonds. The OH bonds can be formed in our

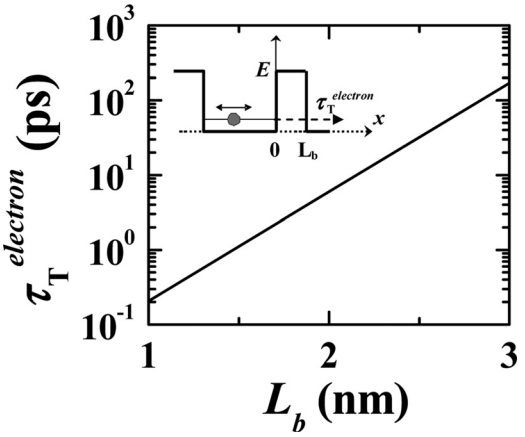

FIG. 4. The barrier thickness (L_b) dependence of calculated tunneling time of electron ($\tau_T^{electron}$). An inset illustrates the semi-classical tunneling model.

fabrication process because the samples were annealed in H_2 for the purpose of eliminating dangling bonds after the NB treatment. If we assume an additional native oxidation barrier with the thickness of only 0.5 nm on the surface of each Si ND, for instance, the tunneling rate becomes longer (32 ps). Therefore, it is reasonable that the PL decay time τ_3 is dominated by the electron transfer.

The picosecond PL component can also be affected by fast non-radiative recombination trapped by surface/interface defects. However, if the non-radiative recombination is dominant, the PL decay time increases at high excitation powers because of filling effects for the limited number of the defect sites. In our case, the decay times of three PL components are almost constant as the excitation power increases; therefore, the fast PL components cannot be explained by the non-radiative recombination. The fast PL decay times in Si QDs were also discussed in terms of an Auger recombination process. The time-dependent spectral variation was observed in previous studies,[6,7] in which fast PL components were attributed to the Auger process. In our case, the excitation power-density was far from the condition that the multiple-exciton generation process governed the PL dynamics. The PL spectrum also did not depend on the delay time after the pulsed excitation and not change with increasing the excitation power. Therefore, we exclude effects of the Auger interaction.

We studied the picosecond dynamics of photo-excited carriers in high-density 2-dimensional Si-ND arrays embedded in SiO_2, which were fabricated by combining a bio-nano-process with NB etching. The PL time-profiles showed triple-exponential decaying kinetics mainly in the picosecond time region. We investigated the disk-density and excitation-power dependences of the PL time-profiles. The fastest PL component (40 ps) was observed only in the high-density Si-ND array sample. We attribute this fast PL component to the electron transfer among the NDs. These optical properties of efficient PL generated in the picosecond time domain motivate one to apply this defect-free high-density Si-ND array to future photovoltaics and optoelectronics based on a platform of the Si integration technology.

This work is supported in part by the Japan Society for the Promotion of Science, Grant-in-Aids for Scientific Research (S) No. 22221007, and Challenging Exploratory Research.

[1]L. T. Canham, Appl. Phys. Lett. **57**, 1046 (1990).
[2]L. Pavesi, L. Dal Negro, C. Mazzoleni, G. Franzo, and F. Priolo, Nature (London) **408**, 440 (2000).
[3]G. Conibeer, M. Green, R. Corkish, Y. Cho, E.-C. Cho, C.-W. Jiang, T. Fangsuwannarak, E. Pink, Y. Huang, T. Puzzer, T. Trupke, B. Richards, A. Shalav, and K.-l. Lin, Thin Solid Films **511–512**, 654 (2006).
[4]C. Eun-Chel, P. Sangwook, H. Xiaojing, S. Dengyuan, C. Gavin, P. San-Cheol, and G. Martin, Nanotechnology **19**, 245201 (2008).
[5]W. Xiaoming, L. V. Dao, and P. Hannaford, J. Phys. D: Appl. Phys. **40**, 3573 (2007).
[6]F. Trojánek, K. Neudert, M. Bittner, and P. Malý, Phys. Rev. B **72**, 075365 (2005).
[7]W. D. A. M. de Boer, D. Timmerman, K. Dohnalova, I. N. Yassievich, H. Zhang, W. J. Buma, and T. Gregorkiewicz, Nat. Nanotechnol. **5**, 878 (2010).
[8]M. Sykora, L. Mangolini, R. D. Schaller, U. Kortshagen, D. Jurbergs, and V. I. Klimov, Phys. Rev. Lett. **100**, 067401 (2008).
[9]Y. Kanemitsu, Phys. Rev. B **53**, 13515 (1996).
[10]I. Sychugov, R. Juhasz, J. Valenta, and J. Linnros, Phys. Rev. Lett. **94**, 087405 (2005).
[11]K. Kůsová, O. Cibulka, K. Dohnalová, I. Pelant, J. Valenta, A. Fučíková, K. Zídek, J. Lang, J. Englich, P. Matejka, P. Štěpánek, and S. Bakardjieva, ACS Nano. **4**, 4495 (2010).
[12]C. H. Huang, X.-Y. Wang, M. Igarashi, A. Murayama, Y. Okada, I. Yamashita, and S. Samukawa, Nanotechnology **22**, 105301 (2011).
[13]C.-H. Huang, M. Igarashi, M. Woné, Y. Uraoka, T. Fuyuki, M. Takeguchi, I. Yamashita, and S. Samukawa, Jpn. J. Appl. Phys. **48**, 04C187 (2009).
[14]T. Kubota, T. Hashimoto, M. Takeguchi, K. Nishioka, Y. Uraoka, T. Fuyuki, I. Yamashita, and S. Samukawa, J. Appl. Phys. **101**, 124301 (2007).
[15]H. Shibata, Jpn. J. Appl. Phys. **37**, 550 (1998).
[16]M. Igarashi, C.-H. Huang, T. Morie, and S. Samukawa, Appl. Phys. Exp. **3**, 085202 (2010).
[17]D. S. Citrin, Phys. Rev. B **47**, 3832 (1993).
[18]M. Sugawara, Phys. Rev. B **51**, 10743 (1995).
[19]S. Haacke, N. T. Pelekanos, H. Mariette, M. Zigone, A. P. Heberle, and W. W. Rühle, Phys. Rev. B **47**, 16643 (1993).
[20]M. Nido, M. G. W. Alexander, W. W. Ruhle, T. Schweizer, and K. Kohler, Appl. Phys. Lett. **56**, 355 (1990).